LETTERS IN BIOMATHEMATICS
An International Journal

Intercollegiate Biomathematics Alliance

RESEARCH ARTICLE

OPEN ACCESS

# Control Strategies to Contain SARS-CoV-2 in a Data Driven SIR Model for the State of Michigan, USA

Norma Ortiz-Robinson, Cyrus Foster-Bey

Grand Valley State University, Allendale, MI

**ABSTRACT**

In this paper we use a data driven SIR model to capture the dynamics of the spread of the SARS-CoV-2 pandemic in the state of Michigan, USA before vaccines were available. The model is then used to formulate an optimal control problem in which we perform sensitivity analysis involving vaccine efficacy, capacity, and hesitancy. We obtain numerical approximations for best strategies for vaccination, treatment, and social distancing measures and their effect on the spread of the virus.

**ARTICLE HISTORY**
Received March 30, 2021
Accepted August 24, 2021

**KEYWORDS**
modeling, optimal control, COVID-19, SIR

## 1 Introduction

Pathogenic RNA viruses are one of the most important groups involved in zoonotic disease transmission and they represent a challenge for global disease control. Their biological diversity and rapid adaptive rates have proven difficult to overcome and to anticipate by modern medical technology (Carrasco-Hernandez, 2017). A commonly known example of a pathogenic RNA virus is influenza. RNA viruses show remarkable capabilities to adapt to new environments and confront the different selective pressures they encounter. Selective pressures on viruses not only include their host's immune system and defense mechanisms, but also the current artificial challenges devised by the biomedical community (i.e. the deployment of drugs and vaccines). Their peculiar rate of adaptive evolution arises from their exceptionally high mutation rates (Carrasco-Hernandez, 2017).

Corona viruses (CoVs) are the largest group of viruses belonging to the *Nidovirales* order. All viruses in the Nidovirales order are enveloped, non-segmented positive-sense RNA viruses (Fehr and Perlman, 2015). Corona viruses usually cause mild to moderate upper-respiratory tract illnesses like the common cold. However, Coronavirus disease 2019 (COVID-2019) is among new corona viruses that have emerged from animal reservoirs to cause serious and widespread illness and death. It is known as Severe Acute Respiratory Syndrome Coronavirus 2 (SARS-CoV-2) (Indwiani and Ysrafil, 2020).

In our work, we will consider an optimal control problem with evolution dynamics derived from the classic SIR model, which divides a given population into three compartments; Susceptible (S), Infected (I), and Removed (R).

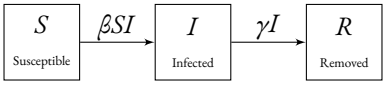


**Figure 1:** Basic SIR model schematic.

As can be observed from the schematic, our SIR model is characterized by two parameters, $\beta$ and $\gamma$, that represent the disease transmission and removal rates respectively. For simplicity of analysis of the optimal control problem we plan to derive, our model ignores birth and non-agent related death rates. Our work will estimate $\beta$ and $\gamma$ using data related to the spread of the virus in the state of Michigan, USA. The goal is to capture the trends of the virus spread in the Michigan population under unchanged conditions. With this knowledge we cast an optimal control problem with mixed constraints, i.e., constraints that involve the state variables $(S, I, R)$ and control functions that characterize vaccination $(u_1)$, treatment $(u_2)$ and social distancing efforts $(u_3)$. Our analysis seeks to understand optimal interventions to control the spread of the virus that are specific to the state of Michigan as well as identify the types of interventions that have the greatest effect. The solution to the optimal control problem establishes strategies (controls) that reach the lowest possible level of susceptible in the population at time $T$, minimize the sum total of infected individuals; and do so while using the least amount of intervention (controls) as possible. Constraints in

CONTACT Norma Ortiz-Robinson ortizron@gvsu.edu

our problem allow us to incorporate limits involving the availability of the vaccine, the public's apprehension to the vaccine, and the capacity of the health care system in Michigan. We will expand on other mathematical details of this problem in Section 3.

A significant volume of work has been undertaken in the past year to better understand SARS-CoV-2 given its impact to our world. Optimal control theory and its application to optimal vaccination strategies and treatment has also been widely studied. The literature is plentiful with general studies that establish necessary conditions for optimality, singularity and other properties of optimal controls (see Biswas et al., 2014; Gaff and Schaefer, 2009; Ledzewicz and Schattler, 2011; Neilan and Lenhart, 2010, for example). Our study is different in that it seeks to best understand these optimal strategies specific to trends of the spread of the virus in the state of Michigan. This is important since the virus has affected states and communities in different ways, which can lead to different optimal strategies. Our model is further novel in that it not only includes constraints involving the weekly availability of vaccines, like Biswas et al. (2014) and Neilan and Lenhart (2010), but also adds a constraint to capture the communities' willingness to vaccinate and a control function to capture social distancing strategies. To our knowledge there are currently no models specific to Michigan SARS-CoV-2 that utilize optimal control in order to analyze the best combination of interventions with regards to social distancing, vaccination, and treatment. Our numerical simulation work will study the effects of changes in vaccine effectiveness (Section 4.1), availability (Section 4.2), and hesitancy (Section 4.3).

# 2 A SIR Model for Michigan

## 2.1 The SIR Model

The SIR (or Kermack-McKendrick) compartmentalized model describes a system of coupled nonlinear ordinary differential equations: $S$ represents the susceptible to the epidemiological agent (hereafter simply agent). Next, $I$, corresponds to those infected who were once susceptible and $R$ designates those who have been removed from the previous compartments by either recovering or retiring mortally from the agent (Kermack and McKendrick, 1927). The basic SIR model assumes that the population size is fixed (i.e., no births, no deaths due to disease nor by natural causes) and closed (no immigration or emigration is accounted for). In addition, there is no latent state (a category of exposed individuals), and the duration of infectivity is the same as the length of the disease. It also assumes a completely homogeneous population with no age, spatial, or social structure. All of these assumptions fall short of resembling the complete dynamics of the spread of COVID-19 and as such predictions should be interpreted through the lens of these limitations. The dynamics of the aforementioned compartments may be modeled by a system of ordinary differential equations given by the following:

$$\frac{dS}{dt} = -\beta SI, \qquad \frac{dI}{dt} = \beta SI - \gamma I, \qquad \frac{dR}{dt} = \gamma I, \tag{1}$$

where $t$ represents time measured in weeks. The two positive constants $\beta$ and $\gamma$ represent the disease transmission coefficient and the removed rate, respectively. The fraction $1/\gamma$ is also the average infectious period by an infected. We further assume that recovered individuals become immune in perpetuity. In our work the system is normalized, that is, the parameters are adjusted so that $S + I + R = 1$.

In our analysis we will be interested in two important numbers associated with the model. The basic reproductive number, $R_0$ is given by the multiplication of the contact rate $\beta$ times the average infectious period $1/\gamma$. In a normalized system like ours, this number may also be referred to as the contact number and can be interpreted as the average number of contacts that an infected has while able to infect (Hethcote, 2000). The number $R_0S(t)$ is referred to as the replacement number, the number of secondary cases from a typical infective, and when $R_0S(t)$ goes below one it is an indication that the epidemic is dying out.

## 2.2 Data Driven Parameters

In order to model the Michigan SARS-CoV-2 data, which included cases and deaths, was downloaded from the MDHHS Coronavirus website (MDHHS, 2021). A third party website from the COVID Tracking Project (2021) was used for Michigan time-series recovered data dating back to April 2, 2020. For our work, we determined the number of active cases (actual infectious) per week by calculating $a(t)$ as

$$a(t) = c(t) - \big(d(t) + r(t)\big),$$

where $c(t)$ are the cumulative cases, $d(t)$ and $r(t)$ are cumulative deaths and recovered, respectively. The data was then normalized so that $1 = S + I + R$, with a Michigan state population of 9.9868 million.

Our approximations are made so that the initial values for S, I, and R match our respective data set from April 2, 2020. We then prioritize the fit for COVID-19 cases during weeks 30–40, which are colored green in the top graph in Figure 2. These represent the latest upward trend that began in the late Fall of 2020. There were two reasons to prioritize this data. First, we wanted to capture the upward trend in order to best understand the trends in the spread before vaccinations were available. Second, given that our basic model assumes a constant infection rate, it isn't able to capture the fluctuations in the rate of change

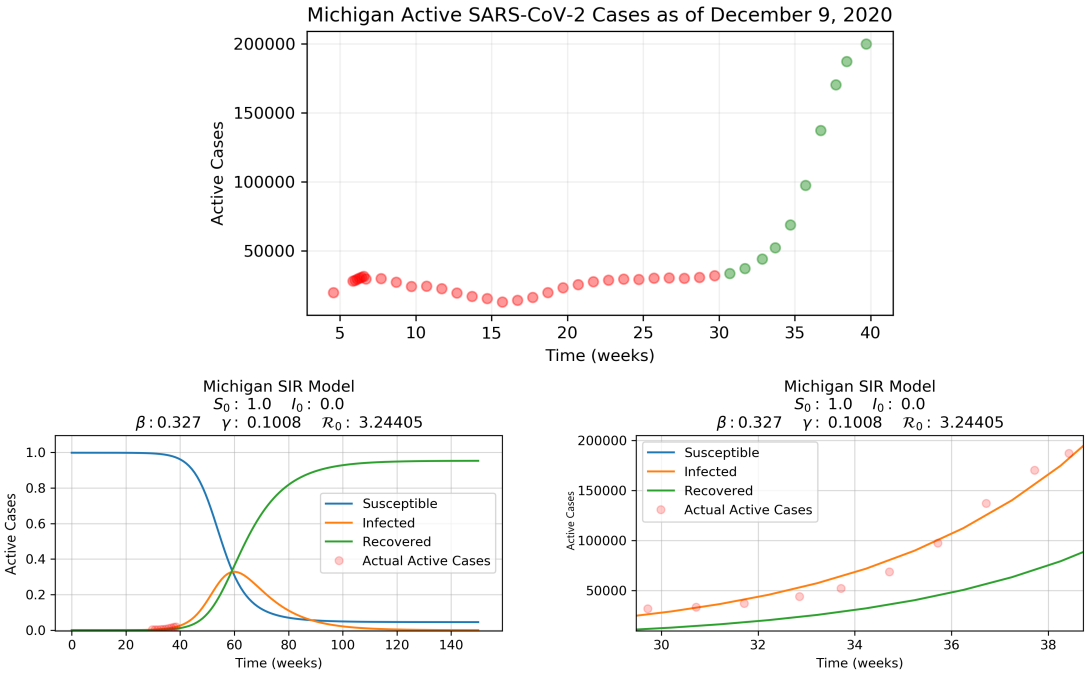


**Figure 2:** SIR modeled Infected versus recent Michigan data (top: Michigan data [selected points for fitting in green]; bottom-left: data fit full-scale; and bottom-right: zoom).

of infections from week to week as observed in the data at the top of Figure 2. To approximate the model parameters, $\beta$ and $\gamma$, we solve the system of differential equations with estimated values and then evaluate the fit accuracy by comparing the values using the mean-squared error (MSE):

$$MSE = \frac{1}{n}\sum_{i=1}^{n}(y - \hat{\mathbf{y}})^2,$$

where $y$ is the vector of observed values and $\hat{\mathbf{y}}$ is the vector of predicted values. Adjustments are made to $\beta$ or $\gamma$ as needed and the process is repeated until the MSE is minimized. Using this method, we achieve parameter values of $\beta = 0.3270$ and $\gamma = 0.1008$ with a MSE of $7.15 \times 10^{-5}$. It is clear from the MSE as well as the graph (see bottom-right graph in Figure 2, that these parameter values capture the general trends of the spread of the virus. We emphasize these parameters are plausible and sufficient for our optimal controls study, but they should not be relied upon as "true" parameters. However, there are examples of parameter approximations that are similar to the ones obtained in this study (see Cooper et al., 2020).

Our estimated parameters indicate then that the average infectious period by an individual is $1/\gamma \approx 9.9206$ days, the basic reproductive number is $R_0 = \beta/\gamma \approx 3.244047$. The last implies the requirement that the susceptible population drop below $1/R_0 \approx 0.30825$ in order to see the epidemic die out.

# 3 The Optimal Control Problem

## 3.1 The Optimal Control Model

We now adjust the SIR model to account for the effects of vaccination ($u_1$), successful treatment ($u_2$), and social distancing measures ($u_3$) with functions $u_1, u_2, u_3$, all of which are time dependent. The new model will thus account for the rates at which a percentage of the population leave the susceptible compartment due to successful inoculation ($e_v u_1 S_1$) where $e_v$ represents the level of efficacy of the vaccine, the infected population is reduced due to treatment ($u_2 I$), and the reduction of the virus transmission rate achieved by social distancing measures ($(1 - u_3)\beta$). These changes are expressed in the schematic shown in Figure 3.

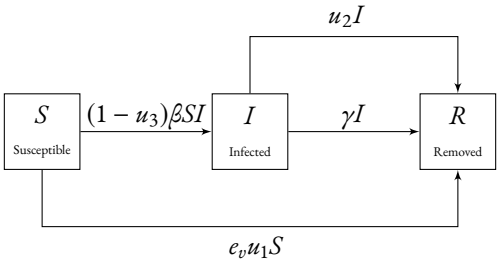


**Figure 3:** SIR model schematic reflecting incorporated controls.

We define the following optimal control problem with mixed constraints (OC-P):

$$\text{Minimize} \quad S^2(T) + \int_0^T AI^2(t) + Bu_1^2(t) + Cu_2^2(t) + Du_3^2(t)\,dt \qquad \text{(Performance Measure)}$$

$$\text{such that:} \qquad (2)$$

$$\frac{dS}{dt} = -(1-u_3)\beta SI - e_v u_1 S \qquad \text{(Dynamics)}$$

$$\frac{dI}{dt} = (1-u_3)\beta SI - \gamma I - u_2 I$$

$$\frac{dR}{dt} = \gamma I + e_v u_1 S + u_2 I$$

$$\frac{dW}{dt} = u_1 S \qquad (3)$$

$$u_1(t)S(t) \le \tau_0 \qquad (4)$$

$$u_2(t)I(t) \le \zeta_0 \qquad (5)$$

$$W(T) \le V_0$$

$$0 \le e_v, u_1, u_2, u_3 \le 1$$

with initial conditions $S(0) = S_0$, $I(0) = I_0$, $R(0) = R_0$, and $W(0) = 0$. The last state equation (3) is introduced so that together with the inequality constraint $W(T) \le V_0$ we may capture the maximum number of susceptible that are willing to receive a vaccine by the end of the treatment time $T > 0$. This state equation is also used in (Biswas et al., 2014) where a discussion of how it may be recast as an integral constraint $\left(\int_0^T u_1(t)S(t)\,dt \le V_0\right)$ as in (Neilan and Lenhart, 2010). Thus $W(t)$ represents the number of susceptible willing to vaccinate in the time period $[0,t]$. The first constraint (4) restricts the amount of vaccine available at each unit of time and will allow us to simulate restrictions in weekly supply of vaccinations. The constant $\tau_0$ represents the maximum availability of vaccine per unit of time (week). The second constraint (5), by contrast, represents the weekly limits of treatment capacity with $\zeta_0$ representing the maximum treatment capacity. It is noteworthy that our approach here incorporates the approach used in (Neilan and Lenhart, 2010) with the extra state equation and (Biswas et al., 2014) with the maximum vaccine load per unit time restriction. However, in (Neilan and Lenhart, 2010) the inequality is used to limit the maximum available vaccine while we assume that vaccines will be unlimited in the long term and only limited on a weekly basis. In addition, inequality (5) is not included in either of the aforementioned analysis.

The performance measure seeks to minimize the total number of infected, the total use of interventions (vaccines, treatment, social distancing) and the final number of susceptible. The constants $A$, $B$, $C$ and $D$ are relative weights that allow us to assign more importance to the minimization of one term versus another.

Throughout we assume that each control $u_i\colon [0,T] \to [0,1]$ is piecewise continuous and the parameter $e_v \in [0,1]$ represents the level of efficacy of the vaccine to produce a sufficient immune response.

## 3.2 Existence of Solutions

Although much of our work will be devoted to numerical simulations involving our optimal control model introduced above, we wish to first establish that the optimal control model admits solutions. To this end, we will first state a general optimal control problem with mixed constraints and a fundamental existence result available for it. To guarantee existence of solutions for our problem (CO-P) we then need only show that it can be seen as a special case of this general problem ($P$).

### 3.2.1 Preliminary existence result

Consider an autonomous (not explicitly dependent on $t$) constrained optimal control problem

$$(P) \qquad \text{Minimize} \quad l(x(T)) + \int_0^T L(x(t), u(t))\, dt$$

subject to:

$$\begin{aligned} \dot{x}(t) &= f(x(t)) + g(x(t))u(t) \\ \mathcal{M}(x(t))u(t) - A_0 &\leq 0 \text{ for all t} \\ u(t) &\in U \text{ a.e. } t \\ x(0) &= x_0 \\ x(T) &\in \mathbb{R}^n \end{aligned}$$

with minimization occurring over all pairs $(x, u)$ with $x\colon \mathbb{R} \to \mathbb{R}^n$ absolutely continuous and $u\colon \mathbb{R} \to \mathbb{R}^m$ Lebesgue measurable. Given that $u(\cdot)$ is only assumed to be measurable, the inclusion is true almost everywhere (a.e.), that is for all $t \in [0, T]$ except some in a set of measure zero. The variable $x$ represents the state and $u$ the controls, both of which may be vectors. In addition, the functions $f$ and $g$ satisfy $f\colon \mathbb{R}^n \to \mathbb{R}^n$ and $g\colon \mathbb{R}^n \to \mathbb{R}^m$, 0 is the $2 \times 1$ vector with zeros in all components, $A_0 \in \mathbb{R}^2$ is a given constant vector, and $\mathcal{M}\colon \mathbb{R}^n \to \mathbb{R}^{2\times m}$. $T$ is fixed and represents the number of weeks since the initial time. Existence of solutions for $(P)$ is established by the following theorem, which is also invoked in (Biswas et al., 2014).

**Theorem 1.** *Suppose that*

*(a) each function $l, L, f, g$, and $\mathcal{M}$ is continuous in $x$,*

*(b) $U$ is a compact set ( in our context this means closed and bounded),*

*(c) given a closed set $C \subset \mathbb{R}^n$, there exists a positive constant $M$ so that $x \in C \Rightarrow |g(x)| \leq M(1 + |x|)$,*

*(c) the function $L(x, u)$ is convex and bounded below,*

*(d) there is at least one pair $(x, u)$ such that $l(x(T)) + \int_0^T L(x(t), u(t))\, dt$ is finite.*

*Then $(P)$ admits a solution pair $(x, u)$.*

The proof of this theorem can be obtained with minimal adjustments from Theorem 23.11 in (Clarke, 2013). See also (Biswas et al., 2014).

### 3.2.2 Existence of solutions for OC-P

In this subsection we offer a proof of existence for our posed optimal control problem (OC-P) that is constructed by showing that (OC-P) is a special case of the stated general problem $(P)$ so that Theorem 1 applies.

**Theorem 2** (Existence of Solutions to OC-P)**.** *As stated, OC-P admits a solution.*

*Proof.* It is enough to show that this problem can be represented by $(P)$ and satisfies the assumptions of Theorem 1 above. Notice that in OC-P, $L(x(t), u(t)) = AI^2(t) + Bu_1^2(t) + Cu_2^2(t) + Du_3^2(t)$ and $l(x(T)) = S^2(T)$ both of which are continuous, convex and bounded below by zero. In addition, the dynamics can be described in the form $\dot{x}(t) = f(x(t)) + g(x(t))u(t)$ by setting $x = [S, I, R, W]^T$, $u = [u_1, u_2, u_3]^T$ and

$$g(x) = \begin{bmatrix} -\beta SI \\ \beta SI - \gamma I \\ \gamma I \\ 0 \end{bmatrix} \qquad \text{and} \qquad g(x(t)) = \begin{bmatrix} -e_v S & 0 & \beta SI \\ 0 & -I & -\beta SI \\ e_v S & I & 0 \\ S & 0 & 0 \end{bmatrix}.$$

It is clear that each $f$ and $g$ are continuous given the continuity of each their entries. The control set $U = [0, 1]$ satisfies the desired compactness. The boundedness assumption $(c)$ of Theorem 1 follows from the fact that each of the components in every term of $g$ as described above is in the set $[0, 1]$. Any solution to the differential equations system will result in a bounded Performance Measure given that every state variable $(S, I, R, W)$ achieves values in the set $[0, 1]$ as do all the control functions. Furthermore, the inequality constraint can be achieved to have the form $m(x(t))u(t) - A_0 \leq 0$ by setting

$$\mathcal{M}(x) = \begin{bmatrix} S & 0 & 0 \\ 0 & I & 0 \end{bmatrix} \qquad \text{and} \qquad A_0 = [\tau_0, \zeta_0]^T.$$

Thus all of the conditions of the theorem are satisfied and we have guaranteed existence of an optimal pair $(x, u)$. □

# 4 Simulations

We now turn our attention to obtaining numerical solutions of our model. We will perform three simulations involving vaccine efficacy, capacity, and hesitancy. Our work uses GEKKO a Python package for machine learning and optimization (Beal et al., 2018). Initial values for the state variables $S$, $I$, and $R$ and the parameters $\beta$ and $\gamma$ are derived from the data with a starting date of April 2, 2020. In all simulations we set $A = 6$, $B = 1$, $C = 1$, and $D = 2$ in an effort to capture the importance of keeping the number of infected as well as social distancing measures ($u_3$) as low as possible. The cost of social distancing can be understood not only as it relates to the discomfort of individuals, but also the socioeconomic challenges of business and school shut downs. We therefore set it to be twice as "expensive" than the cost of treatment and vaccination. We initially considered variations of these relative importance parameters. In our efforts, we did not observe any significant or qualitative changes in optimal strategies when varying the cost of vaccination and treatment ($C$ and $D$). Drastic variations of $A$ and $B$ to prioritize the relative importance of the susceptible versus the infected, did result in changes to optimal treatment given that in the case when $A$ is much larger than $B$ the only way to achieve the lowest possible susceptible is to increase the infective compartment, which is not desirable. In all cases, optimal vaccination strategies did not change and as long as there is a balanced interest in reducing both the infective and susceptible populations, the model generated similar control strategies to the ones with our chosen values for $A$, $B$, $C$ and $D$. More theoretical work could be done in the future to understand exactly how these parameters affect the optimal strategies.

All parameters utilized in our simulations are summarized in Table 1. Numbers with an asterisk represent a default value that will be varied in simulations. The total treatment period of 91 weeks is chosen to understand the spread of the virus through

**Table 1:** Parameters for the normalized SIR model for all of Michigan.

| Parameter | Description | Value |
|---|---|---|
| T | Considered Time | 91 weeks |
| $\beta$ | Disease transmission rate | 0.3270 |
| $\gamma$ | Recovery rate | 0.1008 |
| $e_v$ | Effectiveness of vaccine | 70* |
| $S_0$ | Initial susceptible population | ≈1.000 |
| $I_0$ | Initial infected population | $3.1540 \times 10^{-6}$ |
| $R_0$ | Initial removed population | 0.0000 |
| $V_0$ | Population vaccine acceptance (percent) | 0.70* |
| $\tau_0$ | Maximum vaccine available per week | 0.0185* |
| $\zeta_0$ | Maximum treatment capacity (percent) | 0.0026 |

the end of the year 2021, as many hope that by 2022 life will go back to "normal". In addition, all controls are set to become active after 30 weeks past April 2, 2020 when vaccination became available in Michigan. Prior to 30 weeks all controls are set to zero. The maximum treatment capacity is estimated by using data from the state of Michigan on bed capacity in local hospitals (26,512) and the percentage of the population (70%) willing to receive the vaccine is based on surveys given to the population (see question 14 in EPIC-MRA, 2021).

## 4.1 Vaccine Effectiveness Study

Numerous factors can contribute to the effectiveness of any vaccination program; we focus here on one example. Vaccination has been an effective strategy against influenza infection, however, current preventative vaccines consisting of inactivated virions (chemically deactivated viruses (Sanders et al., 2014)) do not protect all vaccine recipients equally. Typically, influenza vaccines protect 70 to 90 percent of the recipients among healthy young adults and as low as 30 to 40 percent of elderly and others with weakened immune systems (such as HIV-infected or immunosuppressed transplant patients) (Alexander et al., 2004). At the time of writing this article, there are a few vaccines that have been approved and are currently being used in the state of Michigan (Ex. Pfizer, Moderna, Johnson&Johnson) with effectiveness to produce sufficient immune response ranging from 67% to 95% (Mayo Clinic, 2021). In our study we will compare best strategies and outcomes of the model using vaccination efficacy of 30, 70, and 90 percent.

The graphs in Figure 4 show that the vaccination optimal strategy is a bang-bang control. That is to say that it bounces between it's possible allowed extreme values. In this case, it seeks to vaccinate as many as possible for as long as possible and it is zero otherwise. This type of optimal strategy for this problem is supported by the literature in both (Gaff and Schaefer, 2009) and (Biswas et al., 2014). It is not surprising to see the correlation between vaccine efficacy and the number of susceptible at the end of treatment ($S(T)$) as the percentage of susceptible decreasing by 1 for each 1.4–1.5 percent increase in efficacy. However, it is noteworthy that even with a vaccine efficacy of 90%, the percentage of susceptible at the end of the year (34.75%) is above

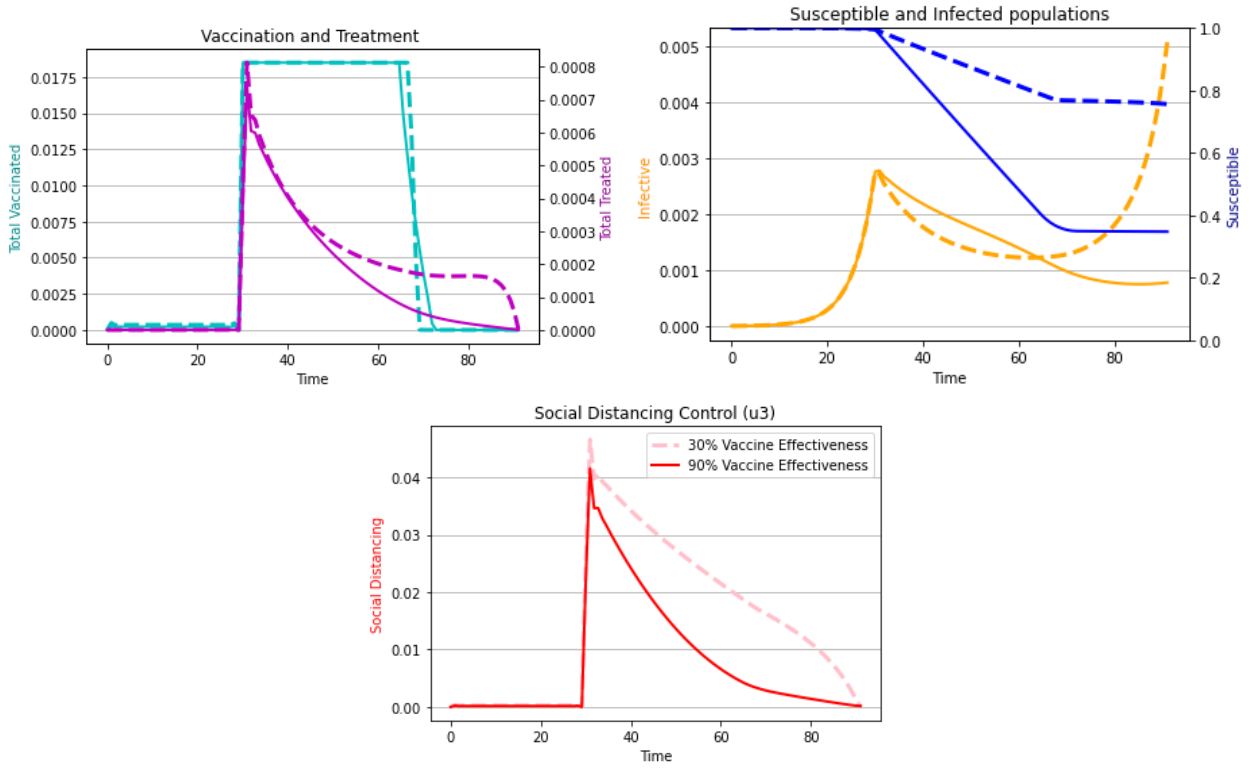


**Figure 4:** Vaccine Effective Study. 30%(−−) vs. 90%( —— ). Weekly vaccination rate: 1.85%, Willingness to vaccinate: 70%.

**Table 2:** Vaccine effectiveness ($e_v$) study. Vaccine efficacy is varied between 30 and 90 percent.

| $e_v$ | $S(T)$ | Total Infected $\times 10^6$ |
|---|---|---|
| 0.9 | 34.75% | 1.1 |
| 0.7 | 48.5% | 1.2 |
| 0.3 | 75.6% | 1.4 |

the desired contact number ratio $1/R_0 \approx 0.30825$ or 30.8% that ends the epidemic. Certainly, 90% vaccine efficacy is helpful and desirable, but under the default values of people willing to vaccinate, it isn't enough to guarantee best outcomes. In terms of social distancing, 30% efficacy of vaccination would require significantly greater social distancing measures that would be expected to continue given the sharp increase seen in the infected population (Upper right, Figure 4). The total number of infected is significant under all scenarios simulated, see Table 2.

## 4.2 Vaccine Capacity Study

We now consider the impact on the spread of the virus if the weekly vaccination rate can be significantly increased. Our default vaccination capacity was selected by considering the apparent weekly vaccination rate in the state as of March of 2021. We contrast this rate with higher rates of vaccination given the likely increase in vaccination capacity and deployment in coming months. We believe the higher 3.7% rate is plausible as it is derived from the following scenario (Campbell and O'Caroll, 2020): Suppose that maximum weekly capacity for dispensing the vaccine is 5,000 per day in a city with a population of 672,662. Statewide that would translate to 74,525 vaccinations per day. If we assume that vaccinations were limited to five days a week (weekdays) the result is 372,625 vaccinations per week. This number represents a weekly vaccination capacity of approximately 3.7 percent of the state's population. Finally, a vaccination rate of 10% is considered. A rate this high would require almost 1 million vaccinations be administered each week in the state of Michigan alone, which we believe to be unrealistic. However, we think it is a good measure of an upper bound for possible outcomes achieved with increased vaccination capacity rates.

The graphs in Figure 5 show that a higher vaccination rate will reach lower susceptible levels sooner. For example, the lowest level is observed to occur in week 40 when the rate is 10% as opposed to in week 70 with a rate of 1.85%. However, in all cases the susceptible population remains approximately within 0.6% from 48%, see Table 3. Without interventions, this level would result

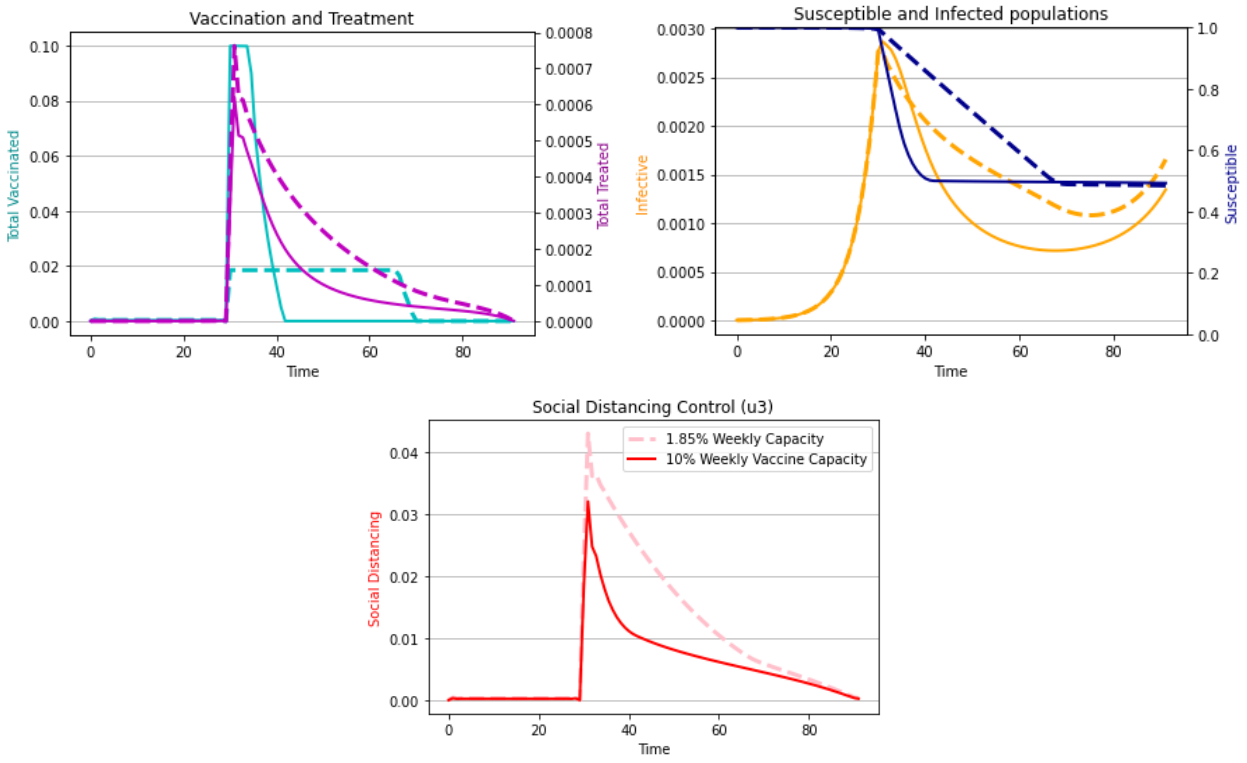


**Figure 5:** Vaccination Rates 1.85%(−−) vs. 10%( —— ). Vaccine efficacy: 70%, Willingness to vaccinate: 70%.

**Table 3:** Vaccine capacity study, varying the maximum allowed weekly rate of vaccination ($u_{1max}$).

| $u_{1max}$ | $S(T)$ | Total Infected $\times 10^6$ |
|---|---|---|
| 0.1 | 49.24% | 0.946 |
| 0.037 | 48.9% | 1.07 |
| 0.0185 | 48.5% | 1.2 |

in the resurgence of the virus and future outbreaks as can be expected from the upward trend in the infective curves. With half of the population still susceptible these scenarios would likely overwhelm available medical services. The total number of infected is significantly impacted implying higher vaccination rates are certainly desirable. The social distancing graphs highlight the significantly higher social distancing measures that would be necessary to sustain for longer periods under the the lowest vaccine capacity regiment.

## 4.3 Vaccine Hesitancy Study

Our last simulation study involves the effects of having more people who are willing to vaccinate. We consider willingness of vaccination at 70, 80, and 90 percent of the population. We do not assume an increase in vaccination rate or efficacy of the vaccine so that both stay at the default 3.7% and 70% respectively.

As the population's willingness to receive the vaccine increases we see a steady decline in the susceptible population at the end of treatment. We observe in Table 4 that, for each 10% increase in the number of vaccinated, we see a 7% decline in the total susceptible at the end of treatment. However, the total susceptible is still above the desired epidemic halting value of 30.8%. The number of infected does stay steady in all three scenarios and optimal social distancing measures appear to be very similar.

## 4.4 Achieving an Epidemic Halting Model

In all of the simulations studied above, the results of optimal strategies resulted in outcomes that in some cases came close to halting the epidemic, though in no case was the outcome enough. In this section, we wish to simulate a combination of what we consider are achievable measures. To that end we will assume a vaccination rate of 3.7%, vaccine efficacy of 90% and at least 80%

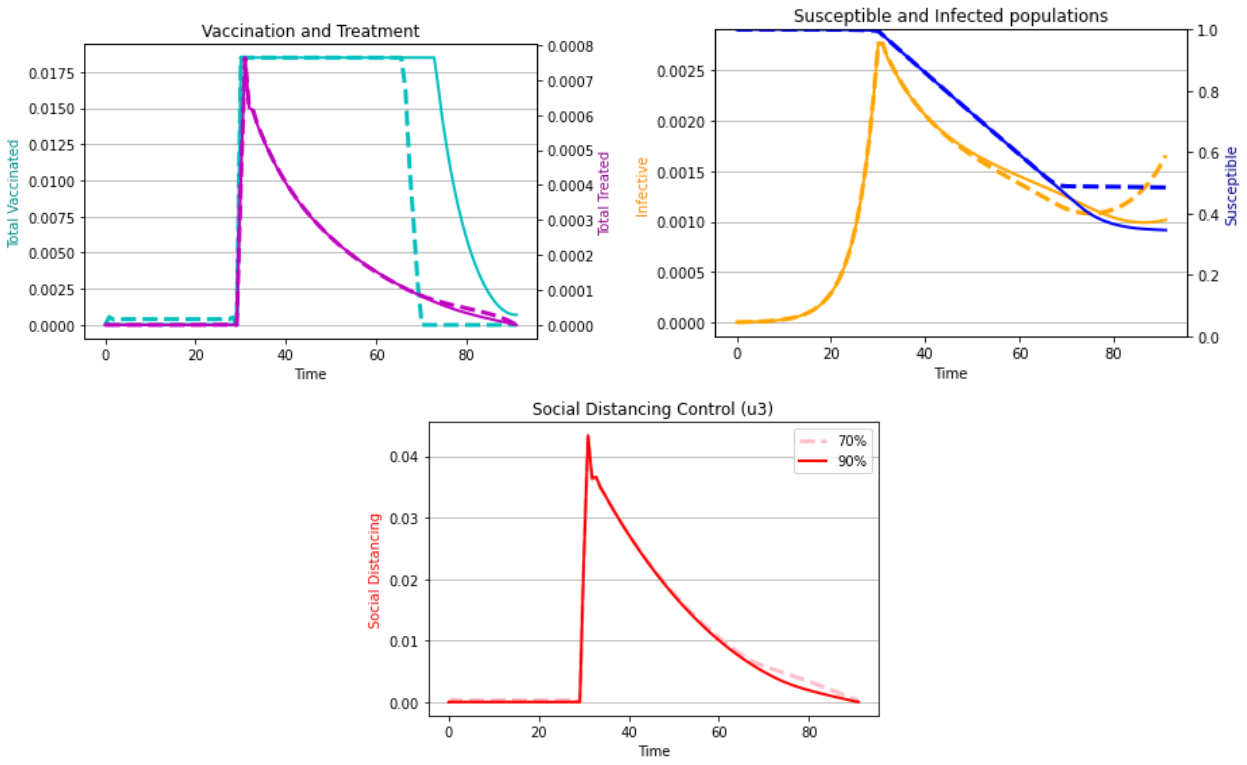


**Figure 6:** Population Willing to Vaccinate Study. 70%(−−) vs. 90%( ——). Vaccine efficacy: 70%, Vaccination rate: 1.85%.

**Table 4:** Vaccine Hesitancy Study. $V_0$: percentage of population willing to receive vaccine.

| $V_0$ | $S(T)$ | Total Infected $\times 10^6$ |
|---|---|---|
| 90% | 34.5% | 1.18 |
| 80% | 41.52% | 1.19 |
| 70% | 48.5% | 1.2 |

of population vaccinates. As noted by the graphs in Figure 7 halting the epidemic becomes possible by the end of the studied time period of 91 weeks.

**Table 5:** Achievable epidemic halting model. $e_v$: vaccine efficacy, $V_0$: percentage of population willing to receive vaccine.

| $e_v$ | $V_0$ | $S(T)$ | Total Infected $\times 10^6$ |
|---|---|---|---|
| 90% | 80% | 26.30% | 0.952 |

In this achievable and optimal scenario, we see the numbers of patients that need treatment reach almost zero around 60 weeks, which in our model corresponds to the summer of 2021. We also observe that the infective curve has a downward trend and that around 53 weeks the susceptible population drops to 26.3%, which allows for the desired $R_0S(T) < 1$. Finally, we see that social distancing measures are near zero at around 55 weeks. Given the dates used and other assumptions of our model, this would correspond to the ability for the population to achieve a more normal lifestyle in the summer of 2021.

We note here that we consider a 90% success rate for the vaccine achievable based on its efficacy to eliminate severe COVID-19 disease. We do not yet know if current results of this efficacy will continue in the future or with the presence of new variants of the virus.

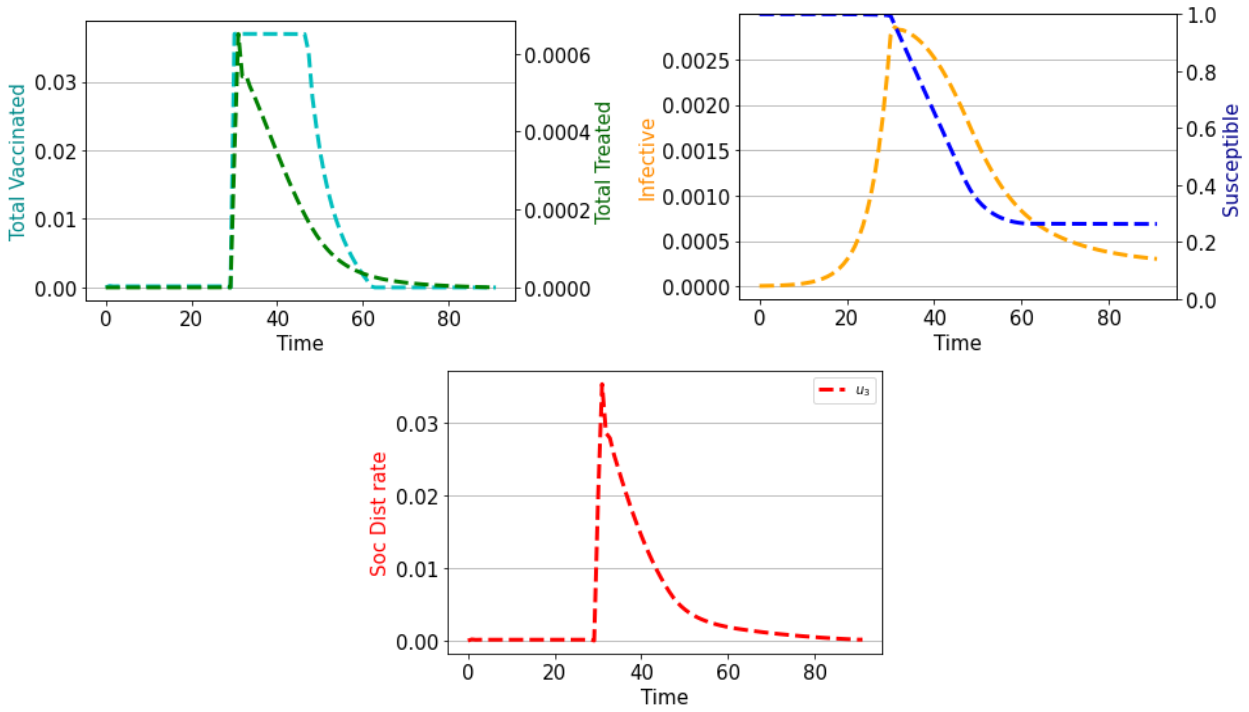


**Figure 7:** Best case scenario considered: Willingness to vaccinate: 80%, Vaccine Efficacy: 90%, Vaccination rate: 3.7%.

## 5 Conclusion

In this article we present a data derived model for the spread of the COVID-19 virus in the state of Michigan that captures the trends of the spread during the surge in infections from late October to December of 2020. An optimal control problem is formulated and simulations are performed to study how changes in vaccine capacity, vaccine effectiveness and vaccine hesitancy affect outcomes and optimal virus deterrent measures. In all cases the optimal vaccine regiment requires that vaccination occur at capacity for as long as there are people left to vaccinate. In addition, we see that the number of infected in all simulations hover between 0.9 million and 1.4 million by the end of the treatment period of 91 weeks.

Our results illustrate that both the vaccine's efficacy to produce an immune response and the percentage of the population willing to vaccinate have the greatest effect in reducing the number of susceptible individuals. The rate of vaccination by contrast, has the greatest effect in the reduction of the total number of infected. We also observe that in all cases the measures simulated are not enough on their own to guarantee a desirable final outcome of control of the spread of the virus since none of the first three scenarios reach the pandemic halting condition that the contact number ratio satisfy $S(t) < 1/R_0$. We did observe that by utilizing improved achievable outcomes for all controls, the model points to a pandemic that can be halted. This is an indication that no one control can work alone, but that instead multiple successful interventions are necessary.

Finally, though our results are not to be interpreted as predictive, they highlight the importance of having multiple successful intervention strategies. In particular, our results point to the important effects of vaccine efficacy and acceptance by the population on virus containment. This qualitative conclusion applies not only to Michigan specifically but to other countries in the world experiencing the pandemic.

## 6 Future Work

In future work we wish to consider another compartment of people who were previously removed but have contracted the virus in order to capture the impact of recent virus variants that may be resistant to current vaccination treatments. From a more analytical perspective, we wish to further study the regularity of the optimal control strategies with regards to singularity and sensitivity to various parameters.

## References


Alexander, M. E., C. Bowman, M. Moghadas, R. Summers, A. B. Gumel, and B. M. Sahai (2004). A Vaccination Model for Transmission Dynamics of Influenza. *SIAM Journal of Applied Dynamical Systems 3*(4), 503–524. 184

Beal, L. D., D. C. Hill, R. A. Martin, and J. D. Hedengren (2018), Gekko Optimization Suit, *Processes 6*(8), 106. doi: 10.3390/pr6080106. 184

Biswas, M. H. A., L. T. Paiva, M. de Pinho (2014). A SEIR model for control of infectuous diseases with constraints. *Mathematical Biosciences and Engineering 11*(4), 781–784. 180, 182, 183, 184

Campbell, D. and L. O'Caroll (November 11, 2020). NHS COVID drive aims to vaccinate up to 5000 people daily at each mass centre. *The Guardian*. https://www.theguardian.com/world/2020/nov/11/thousands-of-hospital-staff-to-be-deployed-in-covid-vaccine-rollout 185

Carrasco-Hernandez, R. (2017). Are RNA Viruses Candidate Agents for the Next Global Pandemic? A Review. *Institute for Lab. Animal Research 58*(3), 343–358. 179

Clarke, F. (2013). *Functional Analysis, Calculus of Variations, and Optimal Control*. New York: Springer-Verlag. 183

Cooper, I., A. Mondal, and C. Antonopoloulos (2020). A SIR model assumption for the spread of COVID-19 in different communities. *Chaos, solitons, and fractals 139*, 110057. doi: 10.1016/j.chaos.2020.110057. 181

The COVID Tracking Project (2021). Last Accessed March 27, 2021. https://covidtracking.com/data/state/michigan 180

EPIC-MRA (2021). EPIC-MRA Poll February 2021. Statewide poll of Active and likely 2022 November voters. Frequent Media. https://www.woodtv.com/wp-content/uploads/sites/51/2021/03/EPIC-MRA-2021-February-SW-Survey-FREQ-MEDIA.pdf 184

Fehr, A. R. and S. Perlman (2015). Coronaviruses: An Overview of Their Replication and Pathogenesis. *Methods of Molecular Biology 1282*, 1–23. 179

Gaff, H. and E. Schaefer (2009). Optimal Control applied to vaccination and treatment strategies for various epidemiological models. *Math. Biosciences and Engineering 6*(3), 469–492. 180, 184

Hethcote, H. W. (2000). The Mathematics of Infectious Diseases. *SIAM Review 42*(4), 599–653. 180

Hethcote, H. W. and S. A. Levin (1989). *Periodicity in Epidemiological Models*. Berlin: Springer.

Indwiani, A. and Ysrafil (2020). Severe Acute Respiratory Syndrome Coronavirus 2 (SARS-CoV-2): An overview of viral structure and host response. *Diabetes & Metablic Syndrome: Clinical Research and Reviews 14*, 407–412. 179

Kermack, W. O. and A. G. McKendrick (1927). A Contribution to the Mathematical Theory of Epidemics. *Proc. of the Royal Society of London A*(115), 700–721. 180

Ledzewicz, U. and H. Schattler (2011). On optimal singular controls for a general SIR model with vaccination and treatment. *Discrete and Continuous Dynamical Systems*, 981–990. 180

Mayo Clinic (2021). Get the Facts about COVID-19 Vaccines. Mayo Clinic. Mayo Foundation for Medical Education and Research. Last accessed March 27, 2021. https://www.mayoclinic.org/diseases-conditions/coronavirus/in-depth/coronavirus-vaccine/art-20484859 184

Michigan Department of Health and Human Services 2021. Last accessed March 27, 2021. https://www.michigan.gov/coronavirus/0,9753,7-406-98163_98173---,00.html 180

Neilan, R. M. and S. Lenhart (2010). An introduction to optimal control with an application in disease modeling. *DIMACS Series in Discrete Mathematics 75*, 67–81. 180, 182

Sanders, B., B. Koldijk, and H. Schuitemaker (2014). Inactivated Viral Vaccines. *Vaccine Analysis: Strategies, Principles, and Control*, 45–80. 184